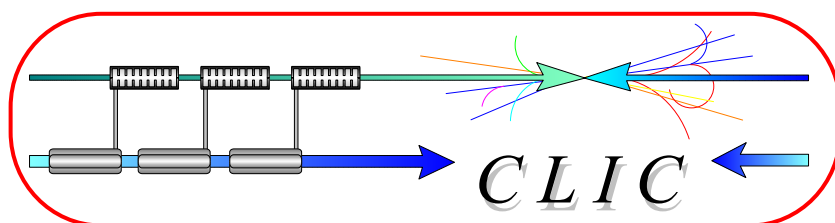


CERN – European Organization for Nuclear Research

European Laboratory for Particle Physics



CLIC Note 472

STUDIES ON THE RF DEFLECTORS FOR CTF3

A. Gallo, D. Alesini, F. Marcellini, INFN-LNF Frascati, Italy
R. Corsini, D. Schulte, I. Syratchev, CERN, Geneva, Switzerland

Abstract

The bunch train compression scheme for the CLIC Test Facility CTF3 relies on the feasibility of fast RF deflectors. They are essentially RF cavities or TW sections working on transverse deflecting mode. The most demanding issues in the deflector design are those related to the beam dynamics, including the beam loading effects on the fundamental deflecting mode, while the efficiency required by the CTF3 parameters can be met by already existing structures. The analysis of the beam dynamics, which addresses the deflector design, is reported in this paper, and different structures representing possible solutions are compared.

Paper presented at the 7th European Particle Accelerator Conference, 26-30 June 2000, Vienna, Austria

Geneva, Switzerland
22 February 2001

STUDIES ON THE RF DEFLECTORS FOR CTF3

A. Gallo, D. Alesini, F. Marcellini, INFN-LNF Frascati, Italy
R. Corsini, D. Schulte, I. Syratchev, CERN, Geneva, Switzerland

Abstract

The bunch train compression scheme for the CLIC Test Facility CTF3 relies on the feasibility of fast RF deflectors. They are essentially RF cavities or TW sections working on transverse, deflecting mode. The most demanding issues in the deflector design are those related to the beam dynamics, including the beam loading effects on the fundamental deflecting mode, while the efficiency required by the CTF3 parameters can be met by already existing structures. The analysis of the beam dynamics, which addresses the deflector design, is reported in this paper, and different structures representing possible solutions are compared.

1 INTRODUCTION

The CTF3[1] project is aimed to test on a reduced scale some of the operational basics aspects of the Compact Linear Collider CLIC, including the bunch train compression scheme, which is devised in two stages.

The first stage consists in delaying half of the bunches by making them circulate in a delay line to obtain 5 separate trains from the original one. The second stage consists in interleaving the 5 trains by making them circulate for a different number of turns in a combiner ring and finally extracting a train 10 times shorter and 10 times more intense with respect to the original one.

The injection and the closed bump orbit allowing the multi-turn circulation in the combiner ring are made with a pair of a RF deflectors working at f_{DB} , the Drive Beam (DB) linac frequency, while the injection/extraction in the delay line is based on a RF deflector working at $f_{DB}/2$.

The main parameters of the CTF3 RF deflectors are summarized in Table 1, comparing the characteristics of standing wave (SW) and traveling wave (TW) structures.

A single-cell cavity working in the deflecting TM_{110} mode, obtained by scaling existing design of crab-crossing cavities[2], is a possible SW candidate. A disk-loaded backward waveguide working in the EH_{11} hybrid mode (RF separator) already optimized for beam deflection[3] has been considered as a possible TW solution.

Both type of structures meet the CTF3 efficiency requirements, in the sense that they can deliver the required deflection at expense of a reasonable amount of RF power. A TW structure is more promising concerning beam dynamics issues, since wakefields are supposed to leave the structure faster, due to the lower filling time, but a rigorous computation of the wake is heavier. In the following we report the analysis of the wake generated by the interaction between the beam and the RF separator deflecting mode (beam loading).

Table I: CTF3 RF Deflector Parameters

	Delay line		Combiner ring	
	TW	SW	TW	SW
nom. Energy E_n [MeV]	184		184	
max. Energy E_{max} [MeV]	350		350	
frequency f [MHz]	1499.28		2998.55	
number of cells N_c	10	1	10	1
De-phasing/cell	$2\pi/3$	---	$2\pi/3$	---
total length L [cm]	67	8	33	4
group velocity v_g/c	-0.0244	0	-0.0244	0
phase velocity v_{ph}/c	1	∞	1	∞
filling time τ_F [ns]	90	800	46	800
Shunt impedance $R_s = (E\phi)^2/2P_{RF}$ [k Ω]	275	300	190	300
Deflection ϕ [mrad]	10		5	
max RF Power P_{RF} [MW]	22	20.5	8	5.1

2 BEAM LOADING IN RF SEPARATORS

The RF separator fields in cylindrical coordinates (r, ϑ, z) in the region inside the irises ($r \leq a$) at the resonant frequency ω^* ($v_{ph} = \omega^*/\beta(\omega^*) = c$) are given by:

$$\begin{aligned}
 E_r &= jE \frac{k^2 a^2 + k^2 r^2}{8} \cos(\vartheta) & H_r &= jE \frac{k^2 a^2 - k^2 r^2 - 4}{8Z_0} \sin(\vartheta) \\
 E_\vartheta &= jE \frac{k^2 r^2 - k^2 a^2}{8} \sin(\vartheta) & H_\vartheta &= jE \frac{k^2 a^2 + k^2 r^2 - 4}{8Z_0} \cos(\vartheta) \\
 E_z &= \frac{E}{2} kr \cos(\vartheta) & H_z &= -\frac{E}{2Z_0} kr \sin(\vartheta) \quad (1)
 \end{aligned}$$

where E is a field scale factor proportional to the square root of the RF power flow in the structure. A charge q crossing the gap in-phase with the deflecting field undergoes a constant Lorentz force $F_\perp = qE/2$. At frequencies $\omega \neq \omega^*$ the field distribution of the mode EH_{11} becomes much more complicated[4] and may be generically indicated as $\underline{E}^0(\omega)$, $\underline{H}^0(\omega)$.

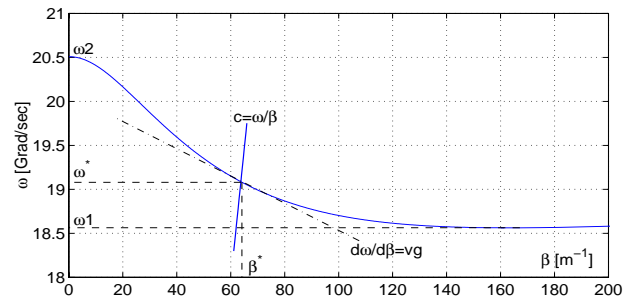


Fig. 1: Dispersion curve of the RF separator EH_{11} mode.

The dependence of the angular frequency ω upon the propagation constant β is shown in the dispersion curve

of Fig. 1. The negative group velocity value reported in Tab. 1 is the derivative of the dispersion curve at ω^* .

The beam loading in transverse, deflecting structures may be described by two mechanisms:

- A. The transverse component of the bunch velocity couples with the deflecting E-field, and the energy exchange creates a deflection gradient along the train;
- B. The longitudinal component of the bunch velocity couples with the longitudinal E-field, which is non-zero off axis, and the energy exchange generates an out-of-phase component of the deflecting field.

The first contribution is very similar to the loading of a linac accelerating section, and the deflection spread along the train can be estimated obtaining a quite small value in our case.

The second contribution is of more concern, because in the combiner ring the bunch pattern is such that at a certain time the deflector will be crossed by bunch trains with a phase separation of only $2\pi/5$, generating a mutual perturbation mainly through the out-of-phase wake. Turn-by-turn the perturbation propagates with the one-turn transport matrix of the ring, and the overall effect may lead to a magnification of the injection errors.

3 SINGLE PASSAGE WAKE

Let's consider a charge q crossing the gap along a certain trajectory. The current density $\underline{J}(t)$ and its Fourier transform $\underline{J}(\omega)$ are given by:

$$\underline{J}(t) = q\delta\left(t - \frac{s}{c}\right)\delta(x')\delta(y') \underline{s}_0(s) \quad (2)$$

$$\underline{J}(\omega) = q e^{-j\omega\frac{s}{c}}\delta(x')\delta(y') \underline{s}_0(s)$$

where s is the distance along the path, \underline{s}_0 is the unit vector tangent to the trajectory, and x', y' are the coordinates on the plane normal to \underline{s}_0 .

The wave excited by $\underline{J}(t)$ is a superposition of the fundamental EH_{11} mode fields $\underline{E}^0(\omega)$, $\underline{H}^0(\omega)$ weighted by the spectral density coefficient $c^+(\omega, z)$ given by[5];

$$c^+(\omega, z) = \frac{\int (\underline{E}_\perp^0(\omega) - E_z^0(\omega) \underline{z}_0) \cdot \underline{J}(\omega) e^{j\beta(\omega)z} dV}{2 \int_{S_1} \underline{E}_\perp^0(\omega) \times \underline{H}_\perp^0(\omega) \cdot \underline{z}_0 dS_1} \approx -\frac{q}{4P(\omega)} \int_z E_z^0(\omega) \Big|_{\substack{\text{particle} \\ \text{trajectory}}} e^{-j\omega z/c} e^{j\beta(\omega)z'} dz' \quad (3)$$

where $P(\omega)$ is the flux of the Poynting's vector and the suffix "+" indicates that the wave has a positive phase velocity. Since we are mainly interested in the out-of-phase beam loading, eq. 3 has been obtained assuming that the current density and the EH_{11} mode interact essentially through their longitudinal components.

Returning in the time domain, the wave excited by a

charge crossing the deflector is given by:

$$\begin{aligned} \underline{E}^+(t, z) &= \frac{1}{\pi} \text{Re} \left[\int_0^{+\infty} c^+(\omega, z) \underline{E}^0(\omega) e^{-j\beta(\omega)z} e^{j\omega t} d\omega \right] \\ \underline{H}^+(t, z) &= \frac{1}{\pi} \text{Re} \left[\int_0^{+\infty} c^+(\omega, z) \underline{H}^0(\omega) e^{-j\beta(\omega)z} e^{j\omega t} d\omega \right] \end{aligned} \quad (4)$$

The most rigorous evaluation of the single passage wake is obtained by considering the Fig. 1 dispersion curve integrating eq. 4 in the pass-band interval (ω_1, ω_2) . The transverse wake excited by a leading charge deflected along a parabolic trajectory ($x_{in} = x'_{in} = 0$; $x'_{out} = 5 \text{ mrad}$) as probed by particles injected out-of-phase with a delay of $T/4$ and $T/4 + \tau_F/2$ is shown in Fig. 2 (solid line). The longer is the delay, the more synchronous is the wake and the larger is the Lorentz force on the trailing particle.

A significant simplification of the problem is obtained by considering a linear dispersion curve in the pass-band interval. The wake computed under this assumption is shown in Fig. 2 (dashed line) and reasonably agrees with the previous one.

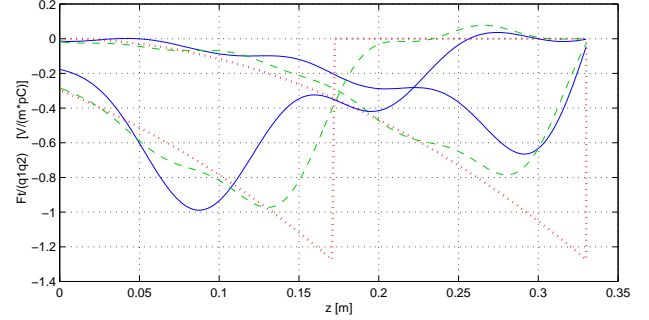


Figure 2: Single passage wakes

A further simplified approach consists in considering only the resonant field configuration of eq. 1 with a local excitation proportional to the leading charge displacement. A rigid wave profile results, which translate backward with the group velocity. The transverse wake calculated with this method, which is far less accurate and physical respect to the previous two, is also shown in Fig. 2 (dotted line). It may be demonstrated that this approach is equivalent to the assumption of a linear dispersion curve over an unlimited frequency range. Anyway, in spite of the different qualitative behavior, the amplitude of this last wake is not too different respect to the other cases.

4 MULTIBUNCH WAKE AND CTF3 COMBINER RING SIMULATIONS

We have considered the effects of the multibunch wake for the bunch pattern of the CTF3combiner ring. The multibunch wake is obtained by simply adding up the single passage wakes taking into account the bunch pattern. After 1 filling time the multibunch wake converges to a regime solution. It is noticeable that the three different single passage wakes of Fig. 2 produce regime multibunch wakes that are almost identical.

The explanation is that the multibunch regime solution is the response to an almost monochromatic excitation, and therefore the details of the dispersion curve out of resonance are not relevant in this case. Therefore the simplest model of single passage wake (corresponding to the dotted line plot of Fig. 2) has been assumed to study the multibunch beam loading in the combiner ring deflectors and, on this base, a simple tracking program has been written to simulate the behavior of the design bunch pattern.

The optical functions at the centre of the deflectors are [6] $\beta_x = 2m$, $\beta_y = 9m$ and $\alpha_x = \alpha_y = 0$. On the side where the beam is injected the phase advance between the deflectors is 180° , while on the other side, where the beam is extracted, it is generically $\Delta\Phi$.

Only the out-of-phase wake of the fundamental EH_{11} mode is included in the simulations and the bunches are point like charges of 2.33 nC separated by 0.1 m in each train. The injected train is put $\Delta z = 0.02$ m ahead of the circulating beam, and 5 trains are merged before the extraction. For the moment only the wake in the horizontal plane has been considered because the vertical one can be detuned by introducing some azimuthal asymmetry in the final deflector design.

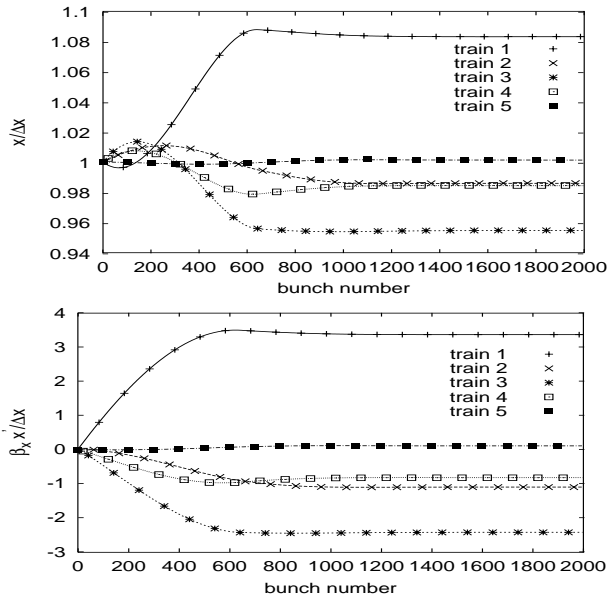


Figure 3: Errors in displacement (a) and angle (b) of the merged trains in the CTF3 combiner ring

The full train after 5 turns for $\Delta\Phi = 180^\circ$ is shown in Fig. 3. The beam had an initial offset $\Delta x = 0.5$ mm and the final positions are not very different from the initial ones (within $-5 \div +10\%$). This is because in the present case, the beam has always the same phase at the reference point. The final angle spread is, however, more significant. In the plot of Fig. 3b the normalized variable $\beta_x x' / \Delta x$ is represented, leading to the conclusion that a magnification of the initial error up to a factor 3 is expected in this case. The strong dependence of the amplification of an initial jitter upon the phase advance

value $\Delta\Phi$ is shown in Fig. 4. The amplifications of an initial offset and that of an initial angle behave similarly. Minima around $\Delta\Phi = 180^\circ$ and $\Delta\Phi = 260^\circ$ are found.

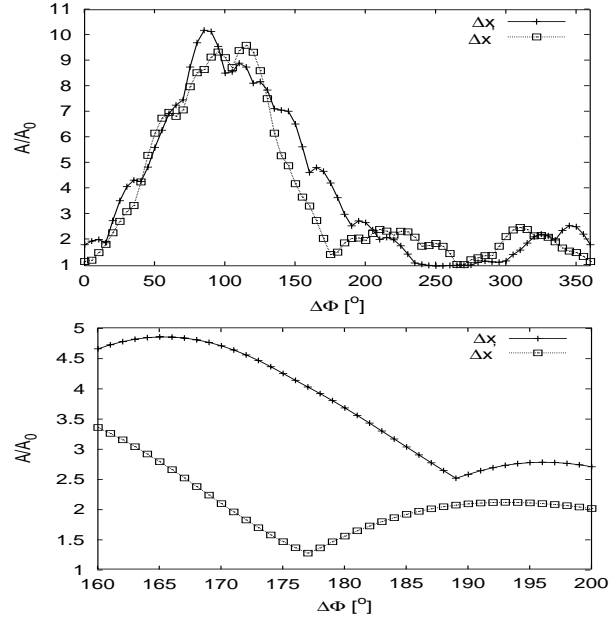


Figure 4: Amplification of an initial error as function of the phase advance $\Delta\Phi$

In the present calculation it is assumed that the deflectors are driven with relatively low power. If more RF power were available, the deflector length could be reduced, which would in turn reduce the wakefield effect.

A first check has also been made on the effects on the beam of the monopole modes in the TW structure case, and the beam energy loss to the first few modes has been found to be negligible.

CONCLUSIONS

Different ways of calculating the single passage wake of the fundamental EH_{11} mode of a RF separator have been compared. The simplest one has been used to make a tracking simulation of the beam loading in the CTF3 combiner ring considering the design bunch pattern.

The simulations show that the amplification of an initial jitter can be minimized by properly choosing the phase advance between the deflectors (i.e. the ring tune). An amplification factor of ≈ 3 is expected for tunes near the integer, which may be an acceptable value. Better results can probably be obtained by exploring the other optimum tune region.

REFERENCES

- [1] H.H. Braun et al., CERN 99-06, 1999.
- [2] K. Akai et al., SLAC-0400, 1992, p.181.
- [3] P. Bernard et al., CERN 68-30, 1968.
- [4] Y. Garault, CERN 64-43, 1964.
- [5] R.E. Collin, "Foundation for microwave engineering", McGraw Hill, 1992.
- [6] C. Biscari et al., THP6B07, this Conference.